Translational Oncology 22 (2022) 101463

Contents lists available at ScienceDirect

Translational Oncology

journal homepage: www.elsevier.com/locate/tranon

Original Research

The role of A-kinase interacting protein 1 in regulating progression and stemness as well as indicating the prognosis in glioblastoma

Jingxia Tang [a,b,c], Shirong Peng [a,b,c], Haifeng Yan [a,b,c], Ming Ni [d], Xiaodan Hou [e], Peizhi Ma [f,g,h], Yuanlong Li [f,g,h,*]

[a] Department of Pharmacy, Children's Hospital Affiliated to Zhengzhou University, Zhengzhou, Henan, China
[b] Department of Pharmacy, Henan Children's Hospital, Zhengzhou, Henan, China
[c] Department of Pharmacy, Zhengzhou Children's Hospital, Zhengzhou, Henan, China
[d] Department of Clinical Pharmacy, Fuwai Central China Cardiovascular Hospital, Zhengzhou, Henan, China
[e] Ward of Heart Failure, Fuwai Central China Cardiovascular Hospital, Zhengzhou, Henan, China
[f] Department of Pharmacy, Henan Provincial People's Hospital, Zhengzhou, Henan, China
[g] Department of Pharmacy, People's Hospital of Zhengzhou University, Zhengzhou University, No.7 Weiwu Road, Zhengzhou, Henan 450000, China
[h] Department of Pharmacy, School of Clinical Medicine, People's Hospital of Henan University, Henan University, Zhengzhou, Henan, China

ARTICLE INFO

Keywords:
AKIP1
Glioblastoma multiforme
Malignant behaviors
RNA-seq
Stemness

ABSTRACT

Background: A-kinase interacting protein 1 (AKIP1) is recently implicated in the pathogenesis of several solid tumors, while its role in glioblastoma multiforme (GBM) is largely unknown. Therefore, the current study aimed to investigate the effect of AKIP1 on GBM cell malignant behaviors, stemness, and its underlying molecular mechanisms.

Methods: U-87 MG and A172 cells were transfected with control or AKIP1 overexpression plasmid; control or AKIP1 siRNA plasmid. Then cell proliferation, apoptosis, invasion, $CD133^+$ cell proportion, and sphere formation assays were performed. Furthermore, RNA-Seq was performed in U-87 MG cells. Besides, AKIP1 expression was detected in 25 GBM and 25 low-grade glioma (LGG) tumor samples.

Results: AKIP1 was increased in several GBM cell lines compared to the control cell line. After transfections, it was found that AKIP1 overexpression increased cell invasion, $CD133^+$ cell proportion, and sphere formation ability while less affecting cell proliferation or cell apoptosis in U-87 MG and A172 cells. Moreover, AKIP1 siRNA achieved the opposite effect in these cells, except that it inhibited cell proliferation but induced cell apoptosis to some extent. Subsequent RNA-Seq assay showed several critical carcinogenetic pathways, such as PI3K/AKT, Notch, EGFR tyrosine kinase inhibitor resistance, Ras, ErbB, mTOR pathways, etc. were potentially related to the function of AKIP1 in U-87 MG cells. Clinically, AKIP1 expression was higher in GBM tissues than in LGG tissues, which was also correlated with the poor prognosis of GBM to some degree.

Conclusions: AKIP1 regulates the malignant behaviors and stemness of GBM via regulating multiple carcinogenetic pathways.

Introduction

Astrocytoma is a common central nervous system tumor with a higher incidence in males than in females, with glioblastoma multiforme (GBM) relatively rare but most deteriorative [1,2]. Apart from the traditional options such as tumor resection, radiotherapy, chemotherapy, and other supportive therapies, several novel treatments, including targeted therapies, immune therapy, etc., have also been proposed, benefiting from the great efforts in this field and the technology improvement [3–6]. Even in this context, the general prognosis of GBM is still dismal, with a median survival of 15 months and a 5-year survival rate of less, around 5.5% [3]. Therefore, it is essential to identify new treatment targets to improve GBM management.

A-kinase-interacting protein 1 (AKIP1) regulates cancer growth, metastasis, and drug resistance in several common cancers such as hepatocellular carcinoma, colorectal cancer, cervical cancer, etc. [7–9].

* Corresponding author at: Department of Pharmacy, People's Hospital of Zhengzhou University, Zhengzhou University, No.7 Weiwu Road, Zhengzhou, Henan 450000, China.
E-mail address: liyuanlong011075@126.com (Y. Li).

https://doi.org/10.1016/j.tranon.2022.101463
Received 3 March 2022; Received in revised form 6 May 2022; Accepted 24 May 2022

Furthermore, in clinical settings, AKIP1 is a high expression in cancerous tissues, and its sufficiency correlates with more advanced tumor features as well as a depraved survival profile in several cancers such as tongue squamous cell carcinoma, papillary thyroid carcinoma, clear cell renal cell carcinoma, prostate cancer, etc. [10–13]. In addition, AKIP1 is observed to induce GBM progression and chemoradiation resistance through the regulation of CXCL1 and CXCL8 [14]. These data exhibit the potency of AKIP1 as a treatment target for GBM, while the mechanisms involved are still far from clear.

Therefore, the current study aimed to investigate the effect of AKIP1 on regulating GBM cell malignant behaviors, stemness, and its potential molecular mechanisms.

Methods

Cell culture

Human GBM cell lines, including GB1, U-251 MG, LN18, A172, and U-87 MG, were purchased from the American Type Culture Collection (ATCC, USA) or Japanese Collection of Research Bioresources Cell Bank (JCRB, Japan), respectively. Furthermore, a patient-derived GBM model was also established by obtaining the fresh surgically resected glioblastoma tumor tissue from patients after informed consent, according to the method in a previous study [15]. All the cell lines were cultured in Dulbecco's Modified Eagle's Medium (DMEM) (HyClone, USA), which were supplemented with 10% fetal bovine serum (FBS) (HyClone, USA). The AKIP1 expression in GBM cell lines was detected with quantitative polymerase chain reaction (RT-qPCR) and western blot, with normal human astrocytes purchased from Lonza Group Ltd. (Lonza, Switzerland) serving as control.

Transfection

AKIP1 overexpression (oeAKIP1), negative control (NC) overexpression (oeNC), AKIP1 knock-down (shAKIP1), and NC knock-down (shNC) plasmids were purchased from Shanghai GenePharma Co., Ltd. (Genepharma, China) using the pGPH1 vector or pEX-2 vector, respectively. The plasmids were transfected into U-87 MG or A172 cells by applying FuGENE 6 Transfection Reagent (Promega, USA). After transfection, the oeAKIP1, oeNC, shAKIP1, and shNC cells were generated. Meanwhile, the U-87 MG or A172 cells without transfection were served as normal controls. At 48 h after transfection, AKIP1 expression, cell apoptosis, cell invasion, CD133 positive ($CD133^+$) cell proportion, and sphere formation ability were determined; At 0, 24, 48, and 72 h, cell proliferation was assessed.

RT-qPCR

The total RNA extraction was completed by RNeasy Protect Mini Kit (Qiagen, Germany). Nanodrop 2000 (Invitrogen, USA) was used to quantify the total RNA. The RT Master Mix (Takara, Japan) was applied to complete the transcription of 1 μg of total RNA. The Fast qPCR Mix (Takara, Japan) was adopted to conduct qPCR. To accomplish the calculation of results, the $2^{-\Delta\Delta Ct}$ method was involved. The primers used in RT-qPCR were as follows: AKIP1: forward, 5′ CCCAACCCTTAGTGCTTCCTTC 3′, reverse, 5′ CGACTCGCCTCTGTGATAACG 3′; β-actin: forward, 5′ GGCACCACACCTTCTACAATGA 3′, reverse, 5′ GGATAGCACAGCCTGGATAGC 3′.

Cell proliferation and apoptosis evaluation

The Cell Counting Kit-8 (Sangon, China) and TUNEL Apoptosis Assay Kit (Beyotime, China) were applied to perform cell proliferation and apoptosis assessments. The instructions for kits were strictly followed.

Cell invasion detection

The transwell system was used to evaluate cell invasion. The insert was pre-coated by Matrigel basement membrane matrix (BD, USA). The cells in FBS-free DMEM were seeded into the insert, and the lower chamber was filled with 10% FBS-containing DMEM. The invaded cells were fixed and stained after the insert was incubated for 24 h. The cells were counted under an inverted microscope (Nikon, Japan).

$CD133^+$ cell proportion assessment

In brief, the cells were harvested and stained with FITC linked CD133 antibody (1:20) (Invitrogen, Thermo) at room temperature for 30 min. The cells were then detected by flow cytometer (BD, USA) and analyzed by Flowjo 7.6 (BD, USA).

Sphere formation

The cells were collected and counted. Then, 300 cells were inoculated onto ultra-low attachment plates in a sphere formation medium and incubated for ten days. The number of spheres whose diameter was $>$ 50 μm was counted and analyzed. The sphere formation medium was DMEM/F12 medium containing 20 ng/ml epidermal growth factor (Sigma, USA), ten ng/ml primary fibroblast growth factor (Gibco, USA), and 5 μg/ml insulin (Sangon, China). For the further limiting dilution assay, 5, 10, and 20 cells were seeded into each well (containing the sphere formation medium) for 24 wells and incubated for ten days to assess the sphere formation. Then, the number of wells with sphere formation was recorded, and the percentage of wells (with successful sphere formation) in 24 wells was also calculated. The Extreme Limiting Dilution Analysis (ELDA) was applied to calculate the 1 / stem cell frequency.

RNA sequencing (RNA-seq) and bioinformatic analysis

After 48 h of transfection, the U-87 MG cells (oeNC, oeAKIP1, shNC, and shAKIP1 groups) were collected. Then, following the kit's protocol, the total RNA was isolated with the RNeasy Protect Mini Kit. Next, the concentration, purity, and integrity of RNA were analyzed by the Agilent 2100 (Agilent, USA). Finally, the RNA-seq library construction and sequencing were completed following the methods described previously [16]. The RNA-seq data analysis was accomplished using the R packages (v3.6.3) (https://cran.r-project.org/bin/macosx/). The feature count was adopted to calculate raw data. The DESeq2 was involved in conducting expression normalization and differential expression analysis. The factoextra package and the pheatmap package were used to plot principal component analysis (PCA) plots and mRNAs' heatmap, respectively. The differentially expressed gene (DEG) was defined as mRNAs with fold change (FC) $\geq$2.0 and adjusted *P-value* (BH multiple test correction) $<$0.05. The volcano plot was used to exhibit DEGs. Gene Ontology (GO) and Kyoko Encyclopedia of Genes and Genomes (KEGG) enrichment analyses were carried out by the DAVID web server.

The Venn diagram package was used to complete cross-analysis and select the accordant DEGs, which were defined as: those who upregulated in oeAKIP1 vs. oeNC and downregulated in shAKIP1 vs. shNC or those who downregulated in oeAKIP1 vs. oeNC and upregulated in shAKIP1 vs. shNC. Then GO, and KEGG enrichment analyses were conducted for the accordant DEGs. Two vital carcinogenetic pathways (PI3K/AKT and Notch) were selected for validation by western blot assay 48 h after transfection in the U-87 MG and A172 cells.

Western blot

RIPA lysis (Sigma, USA) was used to lyse cells. Then the protein concentration was quantified with BCA Protein Assay Kit (Sangon, China). After thermal denatured, the protein was separated with 4–20%

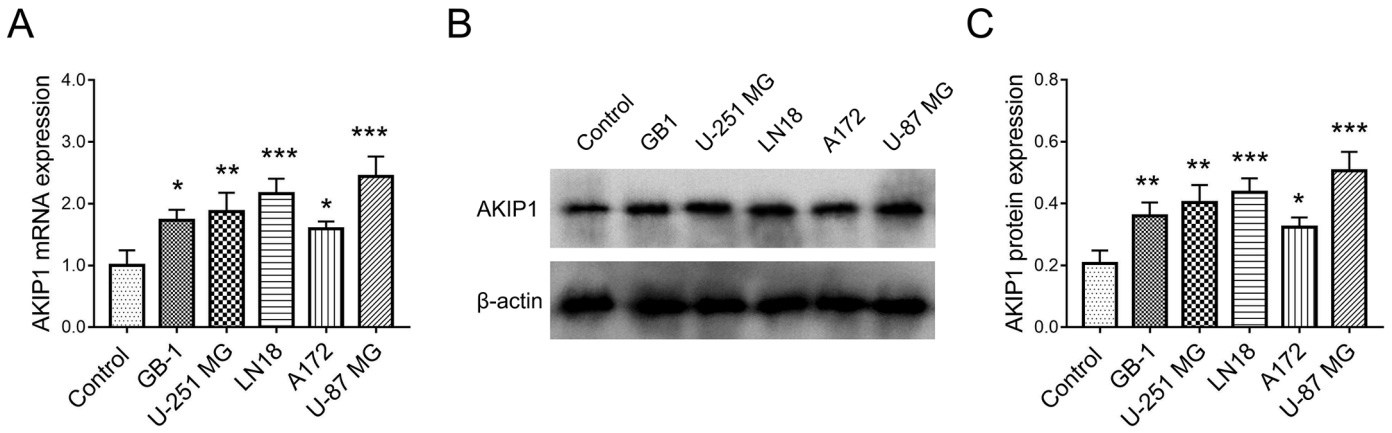

Fig. 1. AKIP1 mRNA and protein expression in GBM and control cell lines. AKIP1 mRNA expression (A) and protein expression (B,C) in GBM cell lines (including GB-1, U-251 MG, LN18, A172, U-87 MG) and control cell lines. Each experiment was replicated three times.

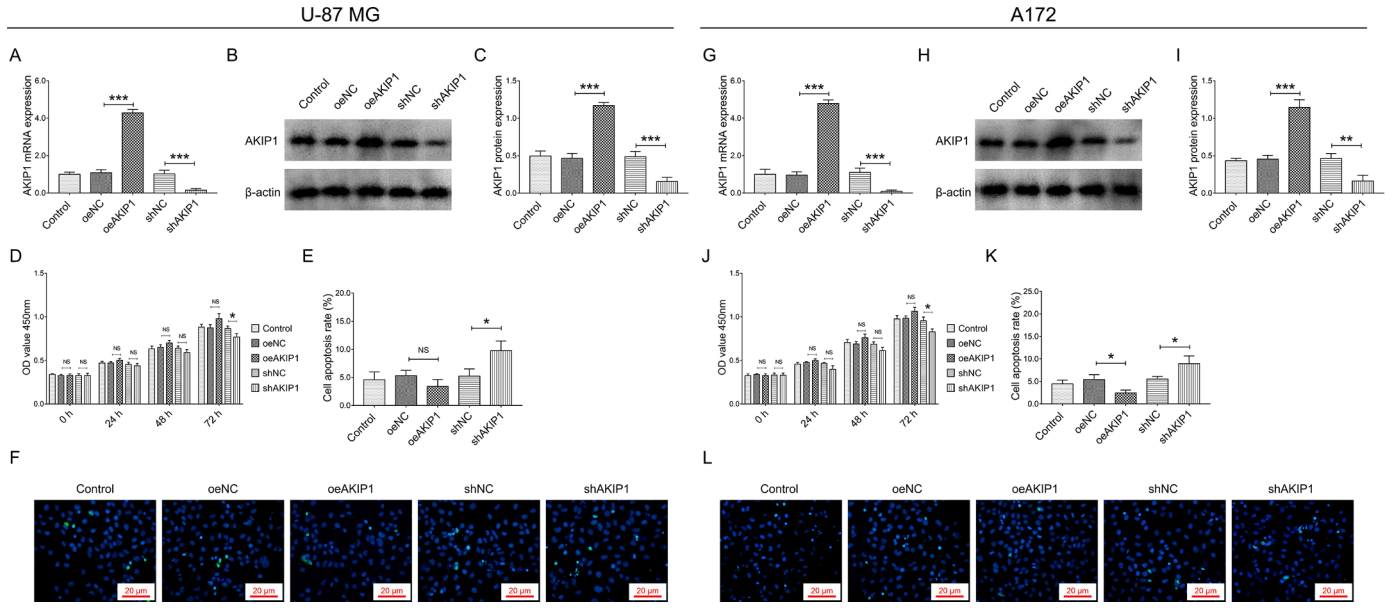

Fig. 2. Effect of oeAKIP1 and shAKIP1 plasmids transfection on cell proliferation and apoptosis in U-87 MG and A172 cell line. The successful transfection of oeAKIP1 and shAKIP1 plasmid was validated by detecting the AKIP1 mRNA (A) and protein (B,C) in U-87 MG cells. The effect of oeAKIP1 and shAKIP1 plasmids transfection on cell proliferation (D) and cell apoptosis rate (E,F) after transfection among groups in U-87 MG cells. The successful transfection of oeAKIP1 and shAKIP1 plasmid was validated by detecting the AKIP1 mRNA (G) and protein (H,I) in A172 cells. The effect of oeAKIP1 and shAKIP1 plasmids transfection on cell proliferation (J) and cell apoptosis rate (K,L) after transfection among groups in A172 cells. Apoptotic cells were fixed with 4% paraformaldehyde fix solution and stained with Tunnel working solution and DAPI staining solution. The bright green color indicated the apoptotic cells. Each experiment was replicated three times.

precast gel (Willget, China) and transferred to nitrocellulose membrane (PALL, USA). The membrane was then incubated with diluted primary antibody at 4℃ overnight and then set with secondary antibody. Protein was visualized using an ECL luminescence reagent (Sangon, China). The antibodies' information was listed in Supplementary Table 1.

Clinical tissue assessment

25 GBM tissues and 25 low-grade glioma (LGG) tissues were obtained from the Department of Pathology. Their clinical data and follow-up data were retrieved after the approval by the Ethics Committee of our institution. Then AKIP1 expression in tissues was detected by immunohistochemistry (IHC) and scored according to the method described in a previous study [14]. The related antibodies and dilutions were as follows: Rabbit anti-AKIP1 antibody (1:100 dilution) (Invitrogen, USA).

The cancer genome atlas (TCGA) database validation

152 GBM patients with available AKIP1, PIK3CA, AKT1, Notch1, and Hes1 mRNA data were downloaded from the TCGA database (available at: https://portal.gdc.cancer.gov/) to further validate the correlation of AKIP1 expression with PIK3CA, AKT1, Notch1, and Hes1.

Statistical analysis

GraphPad Prism 7.02 (GraphPad Software Inc., USA) was used to analyze the data and plot graphs. All data in this study was exhibited as mean and standard deviation. The differences among groups were evaluated by one-way ANOVA followed by Dunnett's or Tukey's multiple comparisons test. The student's *t*-test assessed the differences between the two groups. The Spearman correlation test was carried out for the correlation analysis. The differences in overall survival were exhibited by the Kaplan-Meier curve and determined by the log-rank

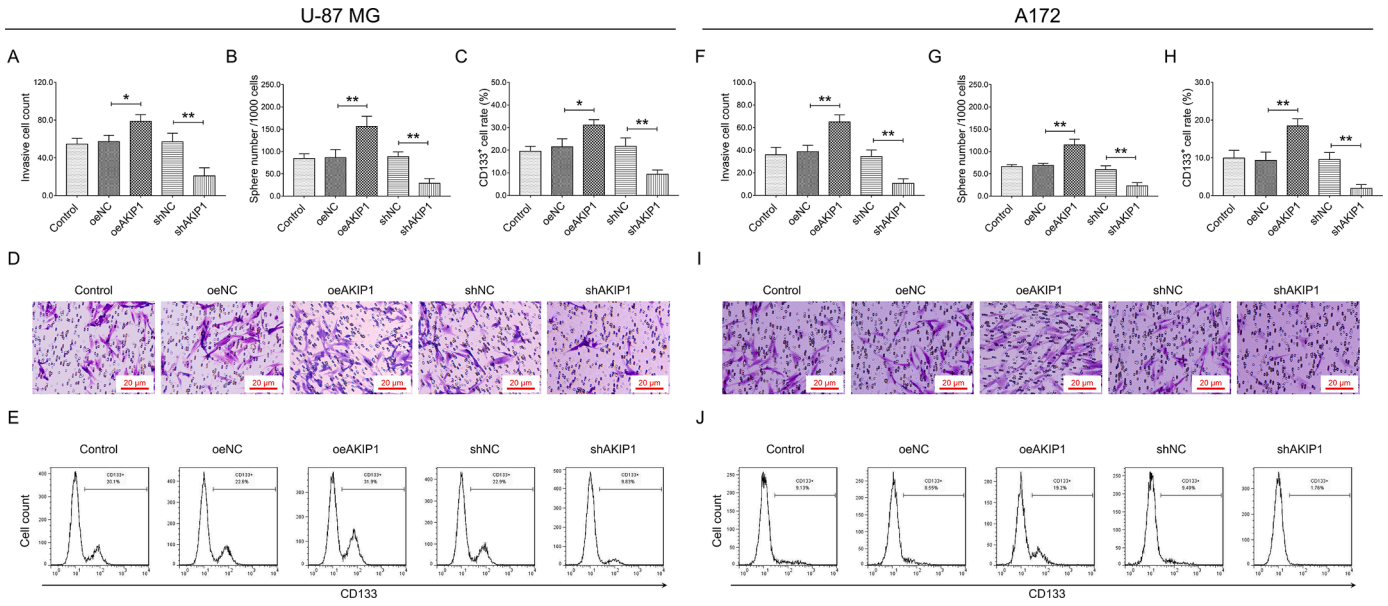

Fig. 3. Effect of oeAKIP1 and shAKIP1 plasmids transfection on invasion and stemness in U-87 MG and A172 cell line. The effect of oeAKIP1 and shAKIP1 plasmids transfection on invasive cell count (A, D), sphere numbers (B), and $CD133^{+}$ cell proportion (C, E) after transfection among groups in U-87 MG cells. The effect of oeAKIP1 and shAKIP1 plasmids transfection on invasive cell count (F, J), sphere numbers (G), and $CD133^{+}$ cell proportion (H, I) after transfection among groups in A172 cells. Invasion cells were fixed with 4% paraformaldehyde fix solution and stained with crystal violet staining solution. The violet color indicated the invasion cells. Each experiment was replicated three times.

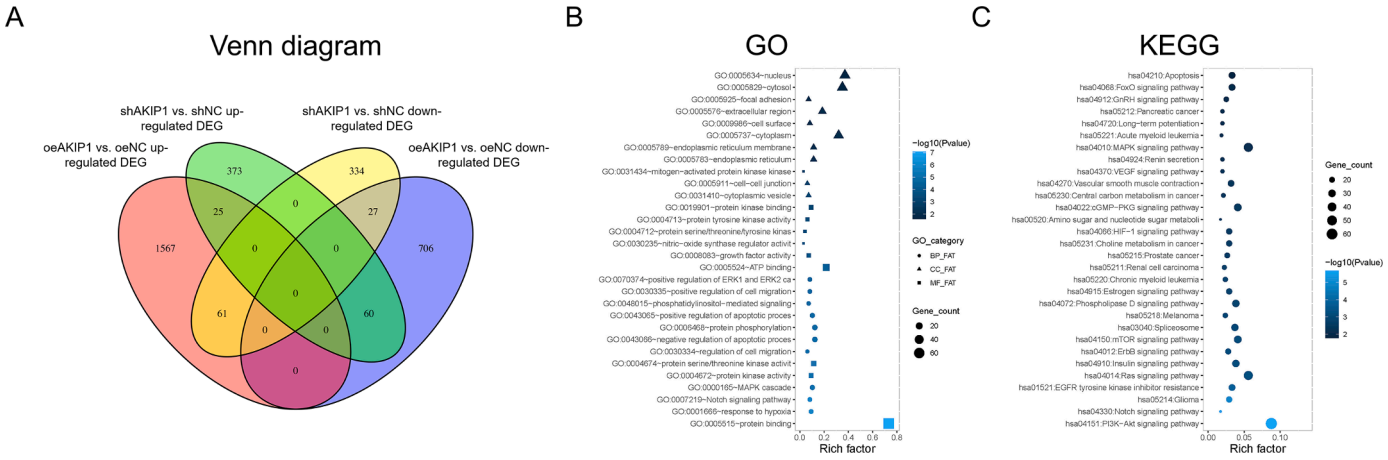

Fig. 4. Cross analysis based on RNA sequencing after oeAKIP1 and shAKIP1 plasmids transfection in U-87 MG cell line. Venn diagram for accordant DEGs between oeAKIP1 and oeNC group; shAKIP1 and shNC group (A): those who upregulated in oeAKIP1 vs. oeNC and downregulated in shAKIP1 vs. shNC, or those who downregulated in oeAKIP1 vs. oeNC and upregulated in shAKIP1 vs. shNC. GO enrichment analysis (B) and KEGG enrichment analysis (C) for accordant DEGs between oeAKIP1 and oeNC group; shAKIP1 and shNC group.

test. The statistical significance was defined as $P < 0.05$. In addition, in the present study, *, **, *** represented $P < 0.05$, $P < 0.01$, and $P < 0.001$, respectively, while NS represented $P > 0.05$.

Results

Effect of AKIP1 modification on GBM cell proliferation and apoptosis

AKIP1 mRNA expressions were higher in GB-1 ($P < 0.05$), U-251 MG ($P < 0.01$), LN18 ($P < 0.001$), A172 ($P < 0.05$), U-87 MG ($P < 0.001$) compared to control cell line (normal human astrocytes, Fig. 1A). In terms of its protein expression, the AKIP1 protein expressions were also higher in GB-1 ($P < 0.01$), U-251 MG ($P < 0.01$), LN18 ($P < 0.001$), A172 ($P < 0.05$), U-87 MG ($P < 0.001$) compared to control cell line (Fig. 1B, C). Then U-87 MG and A172 cell lines were selected for the following experiments.

After the transfection of oeAKIP1, oeNC, shAKIP1, and shNC plasmid into U-87 MG cells and A172 cells, it showed that AKIP1 mRNA was overexpressed in the oeAKIP1 group compared with the oeNC group ($P < 0.001$), and downregulated in shAKIP1 group compared with shNC group ($P < 0.001$, Fig. 2A); besides, the AKIP1 protein was also overexpressed in oeAKIP1 group compared with oeNC group ($P < 0.001$), and downregulated in shAKIP1 group compared with shNC group ($P < 0.001$, Fig. 2B, C); these finding indicated that these transfections were successful. Furthermore, it was noted that three kinds of shAKIP1 plasmids were previously transfected, and the one with the best knockdown effect was chosen for presentation and related experiments. Interestingly, at 0, 24, 48, and 72 h, the cell proliferation rates were of no difference between the oeAKIP1 group compared with the oeNC group (all $P > 0.05$); besides, at 0, 24, and 48 h, the cell proliferation rates were

Table 1
Top 5 pathways.

Pathways	Num of symbols	Symbols	Fold enrichment	*P* value
PI3K-AKT signaling pathway	66	BCL2L11, LPAR6, CDK4, CDK6, CDKN1B, CDC37, COL1A1, COL4A2, CREB1, CSF3, EFNA5, EGFR, EIF4B, EIF4EBP1, AKT1, AKT2, FGF1, FGF5, ITGA11, PHLPP1, MTOR, GNG11, PPP2R3B, ANGPT1, GRB2, HGF, HRAS, IFNAR1, IKBKB, IL4R, IL7, ITGA1, ITGA4, ITGA7, ITGB4, JAK1, KDR, LAMA3, LAMA4, LAMA5, MDM2, MYB, ATF4, NGF, NRAS, PDGFRA, PDGFRB, PGF, PPP2R2A, PPP2R5B, PRKAA1, MAP2K1, MAP2K2, PTK2, RAF1, RPS6, RPS6KB2, SGK1, STK11, TEK, THBS2, VEGFA, YWHAH, PIK3R3, OSMR, EIF4E2	1.815113	2.05E-06
Notch signaling pathway	13	CTBP2, JAG1, DVL3, KAT2A, HES1, RBPJ, LFNG, NOTCH1, NOTCH2, NOTCH4, APH1A, PSEN1, APH1B	2.547346	2.95E-06
Glioma	22	CDK4, CDK6, EGFR, AKT1, AKT2, MTOR, GRB2, HRAS, ARAF, MDM2, NRAS, PDGFRA, PDGFRB, PLCG1, MAP2K1, MAP2K2, RAF1, TGFA, CALM1, CALM2, CALM3, PIK3R3	3.183429	1.3E-05
EGFR tyrosine kinase inhibitor resistance	25	BCL2L11, EGFR, EIF4EBP1, AKT1, AKT2, MTOR, GRB2, HGF, HRAS, ARAF, JAK1, KDR, NRAS, PDGFRA, PDGFRB, PLCG1, MAP2K1, MAP2K2, RAF1, RPS6, RPS6KB2, TGFA, VEGFA, PIK3R3, EIF4E2	2.902958	0.000145
Ras signaling pathway	42	RASGRP1, PAK4, EFNA5, EGFR, AKT1, AKT2, FGF1, FGF5, GNG11, ANGPT1, GRB2, HGF, HRAS, HTR7, IKBKB, KDR, NGF, NRAS, PDGFRA, PDGFRB, PGF, PLA2G4A, PLCG1, PLD1, PRKACB, MAP2K1, MAP2K2, RGL2, RAB5A, RAF1, TEK, TIAM1, VEGFA, CALM1, SHOC2, CALM2, CALM3, BRAP, RASSF5, PIK3R3, RAPGEF5, GAB2	1.732608	0.000603

These pathways were enriched by KEGG enrichment in accordant DEG and displayed by the rank of *p* values. KEGG, Kyoko Encyclopedia of Genes and Genomes; DEG, differentially expressed gene.

also of no difference between shAKIP1 group compared with shNC group (all $P > 0.05$), while at 72 h, the cell proliferation rate was decreased in shAKIP1 group compared with shNC group ($P < 0.05$, Fig. 2D); in terms of the apoptosis results, it showed that the apoptosis rate was similar between oeAKIP1 group and oeNC group ($P > 0.05$), while it was increased in shAKIP1 group compared with shNC group ($P < 0.05$, Fig. 2E, F); these findings disclosed that oeAKIP1 plasmid did not influence U-87 MG cell proliferation and apoptosis, while shAKIP1 plasmid decreased U-87 MG cell proliferation and increased its apoptosis. As for the effect of AKIP1 in A172 cells, similar treads were found among groups as in U-87 MG cells, except for that oeAKIP1 plasmid repressed A172 cell apoptosis (Fig. 2G–L).

Effect of AKIP1 modification on GBM cell invasion and stemness

The invasive cell count was increased in the oeAKIP1 group compared with the oeNC group ($P < 0.05$), while it decreased in the shAKIP1 group compared with the shNC group ($P < 0.01$, Fig. 3A, D); The sphere number/1000 cells was increased in oeAKIP1 group compared with oeNC group ($P < 0.01$), while decreased in shAKIP1 group compared with shNC group ($P < 0.01$, Fig. 3B); The $CD133^+$ cell proportion was increased in oeAKIP1 group compared with oeNC group ($P < 0.05$), while decreased in shAKIP1 group compared with shNC group ($P < 0.01$, Fig. 3C, E); These findings disclosed that oeAKIP1 plasmid overtly promoted invasive cell count, sphere numbers and $CD133^+$ cell proportion in both U-87 MG cell. As for the effect of AKIP1 in A172 cells, similar treads were found among groups as in U-87 MG cells (All $P < 0.01$, Fig. 3F–J). The ELDA analysis was also applied to assess the sphere formation further. The finding showed that: in the U-87 cell line, the oeAKIP1 group disclosed an elevated 1 / stem cell frequency compared with the oeNC group ($P = 0.039$). Besides, the shAKIP1 group also showed an increased 1 / stem cell frequency compared with the shNC group ($P = 0.002$); in the A172 cell line, a similar trend was also observed (both $P < 0.05$; Supplementary Table 2). Furthermore, the effect of AKIP1 modification on GBM cell invasion was further validated in a patient-derived GBM model, which showed that the AKIP1 overexpression increased, while AKIP1 siRNA decreased cell invasion in this patient-derived GBM model (All $P < 0.05$, Supplementary Fig. 1A–D).

RNA-seq findings

To comprehensively explore the potential molecular mechanisms of AKIP1 in GBM, RNA-seq was subsequently performed after transfections in U-87 cells. The detailed bioinformatics findings between oeAKIP1 and oeNC groups, shAKIP1 and shNC groups were shown in Supplementary Fig. 2A–F and Supplementary Fig. 3A–D. The PCA analysis could well differentiate the oeAKIP1 group and oeNC group (Supplementary Fig. 2A). Heatmap analysis exhibited that the internal consistency was satisfying between the oeAKIP1 group and oeNC group; in addition, the cladogram could distinguish the oeAKIP1 group from the oeNC group (Supplementary Fig. 2B). The volcano plot showed that there were 1653 up-regulated mRNAs and 793 down-regulated mRNAs between oeAKIP1 and oeNC groups (Supplementary Fig. 2C). In terms of the shAKIP1 and shNC group, PCA analysis and heatmap showed similar findings (Supplementary Fig. 2D, E); However, the volcano plot analysis showed that there were 458 up-regulated mRNAs and 422 down-regulated mRNAs between the shAKIP1 group and shNC group (Supplementary Fig. 2F). Regarding the GO and KEGG analysis, it indicated that oeAKIP1 vs. oeNC was enriched in various biological processes (such as protein transport, negative regulation of apoptotic process), cellular components (including cytoplasm and mitochondrion), and molecular functions (including RNA binding and ATP binding) (Supplementary Fig. 3A). KEGG analysis revealed that these DEGs were enriched in PI3K-Akt, Ras, and MAPK signaling pathways (Supplementary Fig. 3B). In addition, shAKIP1 vs. shNC was increased in various biological processes (such as negative regulation of the apoptotic process, protein phosphorylation), cellular components (including membrane and cytosol), and molecular functions (including protein binding and ATP binding) (Supplementary Fig. 3C). KEGG analysis revealed that these DEGs were enriched in PI3K-Akt, Ras, and Rap1 signaling pathways (Supplementary Fig. 3D).

Notably, after cross-analysis, the Venn diagram identified 121 DEGs modified by AKIP1 (61 upregulated in oeAKIP1 vs. oeNC and downregulated in shAKIP1 vs. shNC, 60 downregulated in oeAKIP1 vs. oeNC and upregulated in shAKIP1 vs. shNC) (Fig. 4A). Subsequent GO analysis found that these DEGs were enriched in multiple biological processes (such as response to hypoxia, Notch signaling, MAPK cascade, regulation of cell migration, etc.), cellular components (including nucleus,

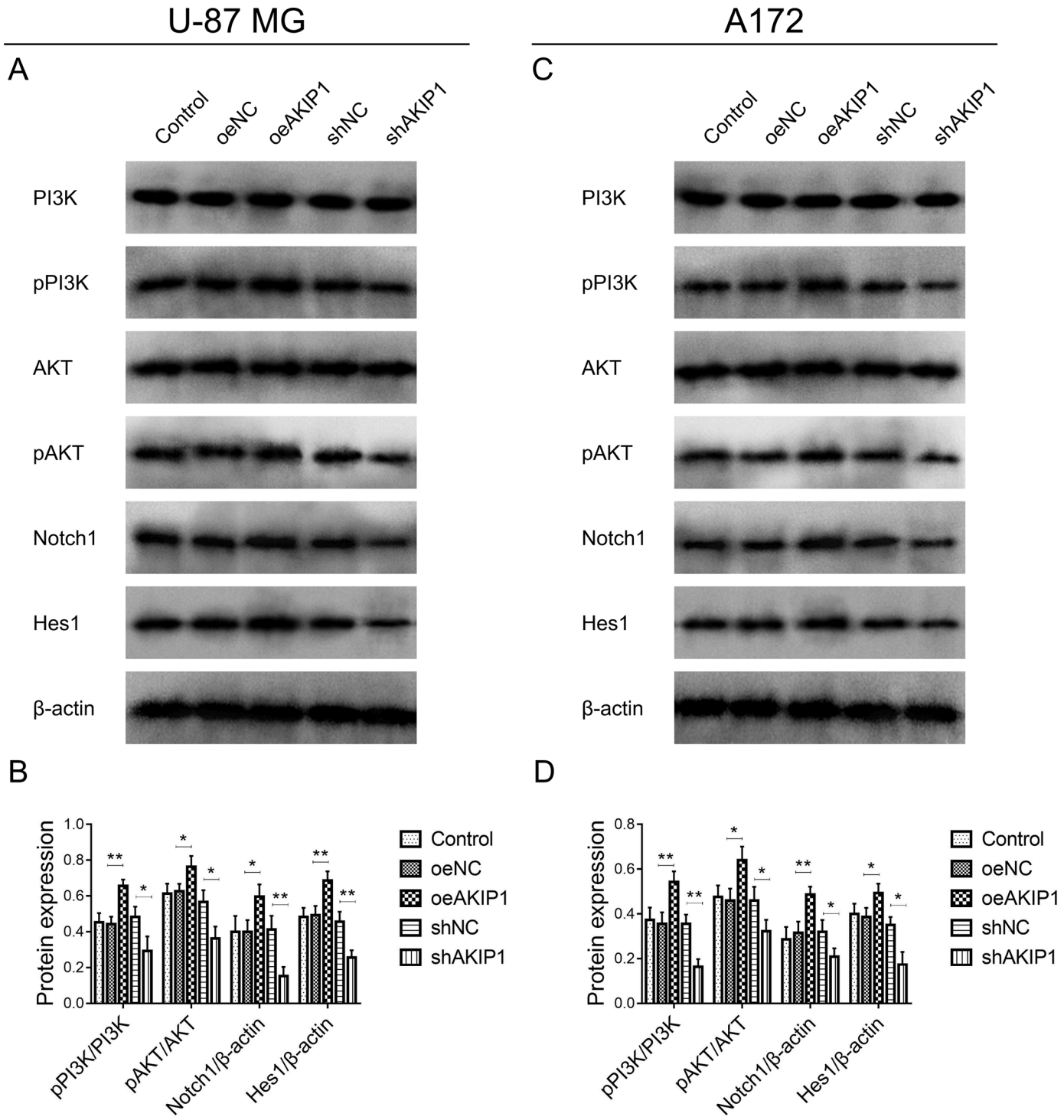

Fig. 5. Effect of oeAKIP1 and shAKIP1 plasmids transfection on PI3K/AKT and Notch pathways in U-87 MG and A172 cell line. Western Blot example (A) and quantifications (B) of PI3K, pPI3K, AKT, pAKT, Notch1, and Hes1 after transfection with oeAKIP1 and shAKIP1 in U-87 MG cells. Western Blot example (C) and quantifications (D) of PI3K, pPI3K, AKT, pAKT, Notch1, and Hes1 after transfection with oeAKIP1 and shAKIP1 in A172 cells. Each experiment was replicated three times.

cytosol, and cytoplasm), and molecular functions (including protein binding and ATP binding) (Fig. 4B). Importantly, KEGG analysis showed that these DEGs were enriched in several key carcinogenetic pathways: PI3K/AKT, Notch, EGFR tyrosine kinase inhibitor resistance, Ras, Insulin, ErbB, mTOR pathways, etc. (Fig. 4C). The detailed enrichment information about the top 5 pathways is exhibited in Table 1.

Validation of PI3K/AKT and Notch pathways

In both U-87 MG and A172 cells, the top 2 involved pathways PI3K/AKT and Notch were further measured by western blot assay. In detail, in U-87 MG cells, pPI3K/PI3K ($P < 0.01$), pAKT/AKT ($P < 0.05$), Notch1/β-actin ($P < 0.05$), and Hes1/β-actin ($P < 0.01$) were elevated in oeAKIP1 group compared with oeNC group ($P < 0.05$), while they were decreased in shAKIP1 group compared with shNC group (all $P <$

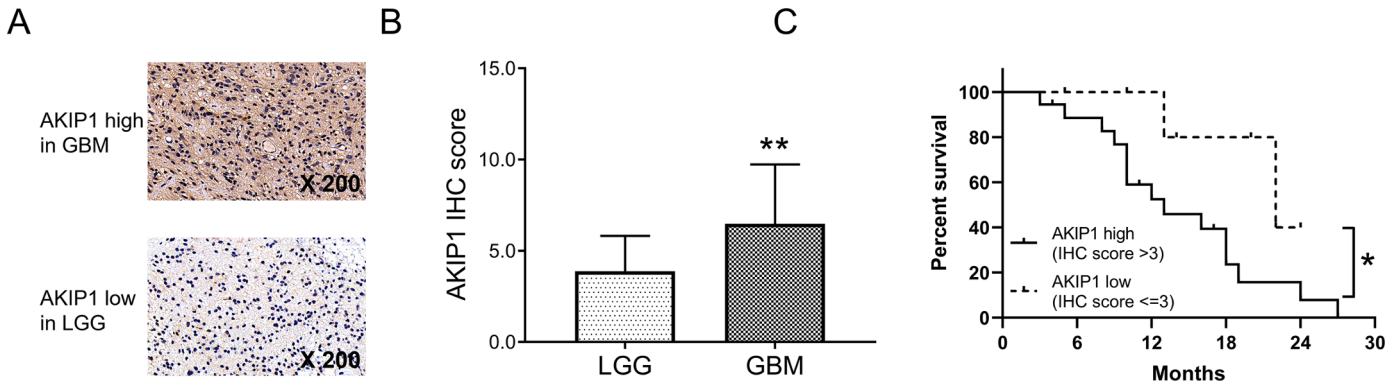

Fig. 6. AKIP1 expression in GBM tissues and its prognostic value in GBM patients. IHC example images (A) and IHC score (B) of AKIP1 between GBM and LGG tissues. Correlation of AKIP1 expression with overall survival in GBM patients (C). GBM and LGG tissue were fixed with 4% paraformaldehyde fix solution and stained with AKIP1 antibody (counterstained with hematoxylin). The brown color indicated the AKIP1 high expression. Each experiment was replicated three times.

0.05, Fig. 5A, B); As for the effect of AKIP1 in A172 cells, similar treads were found among groups as in U-87 MG cells (all $P < 0.05$, Fig. 5C, D). These findings indicated that oeAKIP1 plasmid activated these two pathways while shAKIP1 plasmid inactivated them.

AKIP1 expression in GBM tissue and its clinical value

IHC further examined AKIP1 expression in GBM and LGG tissues, and the AKIP1 IHC score was higher in GBM tissues than that in LGG tissues ($P < 0.01$, Fig. 6A, B). In addition, among these 25 enrolled GBM patients, 18 patients presented with AKIP1 high, while 7 patients exhibited with AKIP1 low. High AKIP1 expression was associated with worse survival in GBM patients ($P < 0.05$, Fig. 6C).

Correlation of AKIP1 with the PI3K/AKT and Notch pathways in TCGA database

AKIP1 expression was positively correlated with PIK3CA ($r = 0.237$, $P = 0.003$, Supplementary Fig. 4A), AKT1 ($r = 0.267$, $P < 0.001$, Supplementary Fig. 4B), and Hes1 ($r = 0.406$, $P < 0.001$, Supplementary Fig. 4D); while it was not associated with Notch1 ($r = 0.081$, $P = 0.317$, Supplementary Fig. 4C).

Discussion

GBM is a critically life-threatening disease worldwide, exhibiting a typical survival duration of 12 to 15 months. Furthermore, in addition to the tumor burden, GBM patients also suffer from non-specific symptoms such as headaches, nausea, stroke, etc. [17,18]. Rapid progression, cancer recurrence, and treatment resistance are the leading causes of the depraved GBM prognosis [3]; therefore, exploring treatment options to inhibit cancer progression, recurrence, and restore treatment sensitivity has never ceased. In addition, cancer stem cells (CSCs) are recently observed to relate to a high risk of recurrence and resistance to treatment in many cancers, including GBM [19–21]. Therefore, observing potential targets for repressing tumor progression and cancer stemness is necessary.

AKIP1 is a recently uncovered oncogene that is involved in tumor cell proliferation, apoptosis, migration, invasion, epithelial-mesenchymal transition (EMT), and related tumor malignant behaviors in several cancers via its regulation on some typical carcinogenic pathways such as NF-κB, AKT, Wnt/β-catenin/CBP, GSK-3β/Snail, etc. [14,22,23]. For instance, AKIP1 promotes cell proliferation, invasion, and EMT *in vitro* and increases metastasis *in vivo* in gastric cancer via modifying Slug [23]; meanwhile, AKIP1 knockdown significantly suppresses cell migration and invasion by blocking Akt/GSK-3β/Snail pathway in breast cancer patients [22]. In addition, AKIP1 induces tumor metastasis and early recurrence in hepatocellular carcinoma via facilitating Wnt/β-catenin/CBP pathway [21]. In the present study, we observed that AKIP1 significantly enhanced cell invasion meanwhile reducing cell apoptosis and increased cell proliferation to some extent in GBM cell lines, as explanations below: (1) AKIP1 promoted a variety of malignant invasion-related genes and pathways, such as NF-κB, AKT, Wnt/β-catenin/CBP, GSK-3β/Snail, and thus improved the GBM cell invasion. (2) GBM cell lines are featured by the extremely high speed of growth and background of high AKIP1 expression; therefore, the AKIP1 overexpression has less effect on cell proliferation and apoptosis, whereas AKIP1 downregulation reduces cell proliferation and induces apoptosis of GBM. Apart from what was mentioned above, another interesting finding is that: disparity in apoptosis findings could be observed after the transfection of oeAKIP1 plasmid into U-87 MG cells and A172 cells. The potential explanation might be as follows: In U-87 MG cells transfected with oeAKIP1 and oeNC plasmid, the dispersion degree of the apoptosis rate is large, which causes a big standard deviation, therefore, the comparison of apoptosis rate between oeAKIP1 group and oeNC group in U-87 MG cells is of no difference. However, in A172 cells transfected with oeAKIP1 and oeNC plasmid, the dispersion degree of the apoptosis rate is small leading to a small standard deviation, which finally causes a statistically significant result.

As for the role of AKIP1 in regulating cancer stemness or CSCs, the studies are far from sufficient. Only one clinical study revealed that AKIP1 was associated with poor pathological differentiation in non-small cell lung cancer patients [24]. Furthermore, some studies found that AKIP1 was related to EMT, drug resistance, cancer metastasis, and recurrence [7,21–23], which were the key features of CSCs or cancer stemness. These imply that AKIP1 might be involved in the regulation of cancer stemness. Our present study found that AKIP1 enhanced cancer stemness in GBM, as evidenced by both the sphere formation assay and $CD133^+$ cell detection. The possible explanations were as follows: AKIP1 regulated some key oncogenetic pathways, such as Wnt/β-catenin, PI3K/AKT, Notch pathways, etc. These pathways are closely engaged in regulating cancer stemness in GBM [25–27].

Regarding the underlying mechanism of AKIP1 in modifying cancer pathogenesis, several molecular experiments have reported that AKIP1 functions as an oncogene via regulating several individual pathways (such as Wnt/β-catenin, AKT, etc.) or oncogenes (such as ZEB1, Slug2, etc.) [7,23,28,29]. However, systemic exploration of the possible molecular etiology of AKIP1 in cancers has been scarcely disclosed, let alone GBM. Our present study conducted RNA-Seq for AKIP1 modification in GBM, then observed that multiple carcinogenetic pathways are involved in the function of AKIP1 in GBM, such as PI3K/AKT, Notch, EGFR tyrosine kinase inhibitor resistance, Ras, ErbB, mTOR pathways, etc., which showed a landscape of potential molecular mechanism of AKIP1 in GBM. Apart from that, it should be noticed that these findings

from this study still need a further *in-vivo* study to verify. Besides, the current research is carried out based on the two traditionally established GBM cell lines and one patient-derived GBM cell line. Only 25 patients are enrolled (the sample size is small); therefore, the limitation of these two aspects is non-neglectable.

Conclusions

In conclusion, AKIP1 promotes the malignant behaviors and stemness of GBM via regulating multiple carcinogenic pathways, implying its potency as a candidate target for GBM treatment.

CRediT authorship contribution statement

Jingxia Tang: Methodology. **Shirong Peng:** Methodology. **Haifeng Yan:** Resources, Data curation. **Ming Ni:** Data curation. **Xiaodan Hou:** Data curation. **Peizhi Ma:** Writing – original draft, Writing – review & editing. **Yuanlong Li:** Visualization.

Declaration of Competing Interest

The authors declare that they have no known competing financial interests or personal relationships that could have appeared to influence the work reported in this paper.

Acknowledgment

This study was supported by Beijing Medical and Health Foundation (No. B17773) and The 23456 Talent Project of Henan Provincial People's Hospital.

Supplementary materials

Supplementary material associated with this article can be found, in the online version, at doi:10.1016/j.tranon.2022.101463.

References

[1] M. Kapoor, V. Gupta, Astrocytoma (2021).
[2] Q.T. Ostrom, D.J. Cote, M. Ascha, C. Kruchko, J.S. Barnholtz-Sloan, Adult glioma incidence and survival by race or ethnicity in the United States from 2000 to 2014, JAMA Oncol. 4 (2018) 1254–1262.
[3] T. Kanderi, V. Gupta, Glioblastoma Multiforme, StatPearls, 2021.
[4] B. Huang, X. Li, Y. Li, J. Zhang, Z. Zong, H. Zhang, Current immunotherapies for glioblastoma multiforme, Front Immunol. 11 (2020), 603911.
[5] T.M. Kinfe, A. Stadlbauer, Y. Bozhkov, N. Kremenevski, S. Brandner, M. Buchfelder, S.R. Chaudhry, The diagnostic and therapeutic role of leptin and its receptor ObR in Glioblastoma multiforme, Cancers (Basel) 12 (2020) 3691.
[6] M. Ziu, B.Y.S. Kim, W. Jiang, T. Ryken, J.J. Olson, The role of radiation therapy in treatment of adults with newly diagnosed glioblastoma multiforme: a systematic review and evidence-based clinical practice guideline update, J. Neurooncol. 150 (2020) 215–267.
[7] Y. Cui, X. Wu, C. Lin, X. Zhang, L. Ye, L. Ren, M. Chen, M. Yang, Y. Li, M. Li, J. Li, J. Guan, L. Song, AKIP1 promotes early recurrence of hepatocellular carcinoma through activating the Wnt/beta-catenin/CBP signaling pathway, Oncogene 38 (2019) 5516–5529.
[8] W. Jiang, W. Yang, L. Yuan, F. Liu, Upregulation of AKIP1 contributes to metastasis and progression and predicts poor prognosis of patients with colorectal cancer, OncoTargets Ther. 11 (2018) 6795–6801.
[9] T.H. Leung, H.Y. Ngan, Interaction of TAp73 and breast cancer-associated gene 3 enhances the sensitivity of cervical cancer cells in response to irradiation-induced apoptosis, Cancer Res. 70 (2010) 6486–6496.
[10] Y. Sun, G. Shi, C. Ma, J. Jiao, Y. Liu, Q. Gao, X. Zhang, Q. Feng, Upregulation of a kinase interacting protein 1 in tongue squamous cell carcinoma correlates with lymph node metastasis and poor overall survival, Medicine (Baltimore) 100 (2021) e25278.
[11] L. Zhang, H. Tao, K. Ke, C. Ma, A-kinase interacting protein 1 as a potential biomarker of advanced tumor features and increased recurrence risk in papillary thyroid carcinoma patients, J. Clin. Lab. Anal. 34 (2020) e23452.
[12] H. Peng, R. Zhang, H. Zhang, A-kinase interacting protein 1 high expression correlates with advanced tumor stage and poor overall survival in surgical patients with clear cell renal cell carcinoma, Medicine (Baltimore) 99 (2020) e20742.
[13] J.C. Ge, Y.X. Wang, Z.B. Chen, D.F. Chen, Integrin alpha 7 correlates with poor clinical outcomes, and it regulates cell proliferation, apoptosis and stemness via PTK2-PI3K-Akt signaling pathway in hepatocellular carcinoma, Cell. Signal. 66 (2020), 109465.
[14] D. Han, N. Zhang, S. Zhao, H. Liu, X. Wang, M. Yang, S. Wang, Y. Li, Z. Liu, L. Teng, AKIP1 promotes glioblastoma viability, mobility and chemoradiation resistance via regulating CXCL1 and CXCL8 mediated NF-kappaB and AKT pathways, Am. J. Cancer Res. 11 (2021) 1185–1205.
[15] F. Jacob, R.D. Salinas, D.Y. Zhang, P.T.T. Nguyen, J.G. Schnoll, S.Z.H. Wong, R. Thokala, S. Sheikh, D. Saxena, S. Prokop, D.A. Liu, X. Qian, D. Petrov, T. Lucas, H.I. Chen, J.F. Dorsey, K.M. Christian, Z.A. Binder, M. Nasrallah, S. Brem, D. M. O'Rourke, G.L. Ming, H. Song, A patient-derived glioblastoma organoid model and biobank recapitulates inter- and intra-tumoral heterogeneity, Cell 180 (2020) 188–204, e122.
[16] S.R. Head, H.K. Komori, S.A. LaMere, T. Whisenant, F. Van Nieuwerburgh, D. R. Salomon, P. Ordoukhanian, Library construction for next-generation sequencing: overviews and challenges, BioTechniques 56 (2014) 61–64, 66, 68, passim.
[17] R.M. Young, A. Jamshidi, G. Davis, J.H. Sherman, Current trends in the surgical management and treatment of adult glioblastoma, Ann. Transl. Med. 3 (2015) 121.
[18] Q.T. Ostrom, G. Cioffi, H. Gittleman, N. Patil, K. Waite, C. Kruchko, J.S. Barnholtz-Sloan, CBTRUS statistical report: primary brain and other central nervous system tumors diagnosed in the United States in 2012-2016, Neuro Oncol. 21 (2019) v1–v100.
[19] P.K. Raghav, Z. Mann, Cancer stem cells targets and combined therapies to prevent cancer recurrence, Life Sci. 277 (2021), 119465.
[20] V. Mattei, F. Santilli, S. Martellucci, S. Delle Monache, J. Fabrizi, A. Colapietro, A. Angelucci, C. Festuccia, The importance of tumor stem cells in glioblastoma resistance to therapy, Int. J. Mol. Sci. 22 (2021) 3863.
[21] N. Jing, W.Q. Gao, Y.X. Fang, Regulation of formation, stemness and therapeutic resistance of cancer stem cells, Front. Cell Dev. Biol. 9 (2021), 641498.
[22] D. Mo, X. Li, C. Li, J. Liang, T. Zeng, N. Su, Q. Jiang, J. Huang, Overexpression of AKIP1 predicts poor prognosis of patients with breast carcinoma and promotes cancer metastasis through Akt/GSK-3beta/Snail pathway, Am. J. Transl. Res. 8 (2016) 4951–4959.
[23] D. Chen, G. Cao, Q. Liu, A-kinase-interacting protein 1 facilitates growth and metastasis of gastric cancer cells via Slug-induced epithelial-mesenchymal transition, J. Cell. Mol. Med. 23 (2019) 4434–4442.
[24] Y. Liu, J. Tian, D. Qin, J. Liu, Y. Xie, AKIP1 expression in tumor tissue as a new biomarker for disease monitoring and prognosis in non-small cell lung cancer: results of a retrospective study, J. Clin. Lab. Anal. 34 (2020) e23128.
[25] C.Y. Tsai, H.J. Ko, C.F. Huang, C.Y. Lin, S.J. Chiou, Y.F. Su, A.S. Lieu, J.K. Loh, A. L. Kwan, T.H. Chuang, Y.R. Hong, Ionizing radiation induces resistant glioblastoma stem-like cells by promoting autophagy via the Wnt/beta-catenin pathway, Life (Basel) 11 (2021) 451.
[26] X. Zhang, J. Wang, Y. Wang, G. Liu, H. Li, J. Yu, R. Wu, J. Liang, R. Yu, X. Liu, MELK inhibition effectively suppresses growth of glioblastoma and cancer stem-like cells by blocking AKT and FOXM1 pathways, Front. Oncol. 10 (2020), 608082.
[27] S. Panza, U. Russo, F. Giordano, A. Leggio, I. Barone, D. Bonofiglio, L. Gelsomino, R. Malivindi, F.L. Conforti, G.D. Naimo, C. Giordano, S. Catalano, S. Ando, Leptin and notch signaling cooperate in sustaining glioblastoma multiforme progression, Biomolecules 10 (2020) 886.
[28] D. Ma, M. Li, J. Su, S. Zhang, BCA3 contributes to the malignant progression of hepatocellular carcinoma through AKT activation and NF-kappaB translocation, Exp. Cell. Res. 362 (2018) 142–151.
[29] X. Guo, L. Zhao, D. Cheng, Q. Mu, H. Kuang, K. Feng, AKIP1 promoted epithelial-mesenchymal transition of non-small-cell lung cancer via transactivating ZEB1, Am. J. Cancer Res. 7 (2017) 2234–2244.